

Statistical modeling of spray formation, combustion, and evaporation of liquid fuel droplets

S. Bolegenova¹, A. Askarova¹, N. Slavinskaya², Sh. Ospanova^{1*},
A. Maxutkhanova¹, A. Aldiyarova¹ and D. Yerbosynov¹

¹Al-Farabi Kazakh National University, Almaty, Kazakhstan

²German Aerospace Centre (DLR), Stuttgart, Germany

*e-mail: Shynar.Ospanova@kaznu.edu.kz

(Received 4 October 2022; received in revised form 8 November; accepted 21 December 2022)

This article is devoted to computer simulation of the atomization, combustion, and evaporation processes of liquid fuel drops (heptane) at high turbulence. The paper describes the main characteristics and methods of atomization of liquid fuels and shows the types of special devices used in fuel supply injection systems. As proposed in the paper mathematical model of the combustion of liquid fuel injections at high turbulence consists of the laws of conservation of mass, momentum, transfer of kinetic energy, and conservation concentration of the mixture components. Also, when setting up computational experiments, the chemical model of reacting systems, the turbulence model, and the equations describing evaporation, heat transfer, and interaction with the gaseous medium were taken into account. As a result of the computational experiments performed to study the liquid fuel droplets' injection rate influence on the processes of its spraying and combustion, the optimal combustion mode was established. The obtained data that determine the optimal mode are confirmed by a graphical interpretation of the distribution of temperature fields, the number of combustion products, and particles along the height of the model combustion chamber. These results will contribute to a deep study and construction of the liquid fuels' combustion theory, and an understanding of complex thermal and physical phenomena in combustion chambers.

Keywords: atomization, heptane, injection rate, computational experiment, combustion, evaporation.

PACS number: 07.05.Tp.

1 Introduction

Energy is one of the key sectors of the modern global economy, ensuring economic growth is associated with an increase in energy consumption, while the cost of energy production largely determines the availability of goods and services. The high cost of widely used energy carriers, such as natural gas and high-quality petroleum products, is associated with the depletion of primary energy resources and the insufficient level of their beneficial use. This explains the interest in the use of cheap, low-quality fuels that are not currently in demand by the energy industry. The main reason for the low share of such fuels in the fuel and energy balance is the lack of technologies that meet modern efficiency and environmental safety requirements.

For the thermal power industry, the tasks associated with increasing the efficiency of the use of energy resources are of particular importance.

Currently, an urgent task is the disposal of huge amounts of liquid hydrocarbon waste accumulated in industrial enterprises: used motor and transmission oils, lubricating fluids, oil sludge, waste from oil production, and oil refining. Known liquid fuel combustion technologies do not always provide high combustion efficiency and compliance with environmental standards when using low-grade fuels. Such fuels ignite poorly and emit a significant amount of soot. For their combustion, special designs of burners are required to ensure combustion stability and high completeness of fuel combustion without violating the standards for harmful emissions. The solution to this problem is important both in terms of improving the environmental situation and in order to expand the fuel and raw material base of the energy sector through the use of substandard liquid hydrocarbon fuels.

Of particular relevance are studies aimed at developing the scientific background and

substantiating the development of new devices and technologies that provide high technical and environmental performance in the production of energy using low-quality hydrocarbon fuels, including solving problems of autonomous heat supply for industrial and residential facilities.

Systematic research shows that transport generates about 25-30% of the total CO₂ emissions in the European Union per year. Electromobility projects aim to significantly reduce the carbon footprint of the sector. Strategies to reduce emissions related to the transport sector are about modes of movement and modernization of the transport system. The amount of CO₂ produced by a specific car depends on many factors.

However, when considering the entire transport sector, passenger cars emit the largest amount of carbon dioxide. Road transport accounts for 72% of total emissions, while passenger cars account for up to 60.7%, which is 43.7% of the total [1, 2]. This is significantly more than in maritime (13.6% of the total) or air transport (13.4%). In the coming decades, statistics on emissions from passenger transport are not optimistic: it is expected to remain at the same level or even increase, rather than decrease.

In 2020, the global carbon ratio (CO₂ emissions per tonne of oil equivalent consumed) decreased by

0.9%, significantly more than between 2010 and 2019 (-0.3%/year) [3-5]. This improvement is due both to a significant decrease in oil consumption, which is associated with pandemic-induced quarantine measures and restrictions in the transport sector, and an acceleration in the electricity's decarbonization generation process: a decline in electricity production at "flexible", usually thermal, power plants because of a reduction in energy consumption. Decreasing energy consumption and steady growth in electricity generation from renewable resources have contributed to a reduction in heat generation and reduced consumption of fossil fuels in the energy sector.

The carbon ratio declined in the EU (-4.4%), the US (-3.4%), Canada (-9.5%), Latin America and Africa (-4.4%). In Asia, the situation has changed to a lesser extent (-0.6%), as in China the carbon coefficient has decreased by only 0.5%, since coal consumption is still growing [4, 5]. This indicator went down in India because of declining coal-fired power generation and in South Korea because of increased nuclear power generation but rose slightly higher in Japan and Indonesia. In addition, the carbon ratio decreased in Russia and Australia due to lower coal consumption, as also in the Middle East (Figure 1) [6].

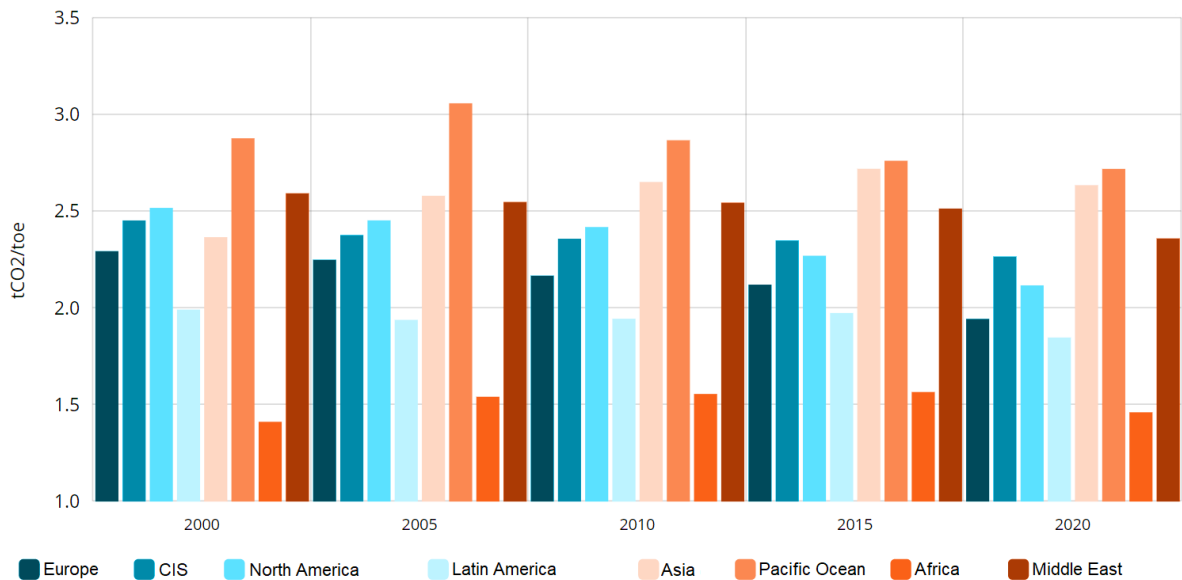


Figure 1 – Evolution trend of the carbon coefficient over the period 1990-2020

When regulating carbon emissions from road transport, it is worth following the European Commission's directives, which are a set of guidelines aimed at reducing carbon dioxide emissions into the atmosphere, including improving the efficiency of the transport system. Improving internal combustion engines and optimizing hydrocarbon fuel combustion processes makes it possible to reduce carbon dioxide emissions.

The concept of convective heat and mass transfer in turbulent currents with chemical reactions is widespread and plays a major role in natural processes as well as in various industries. Knowing the laws of such flows is important in building a theory of combustion physics, in creating new physical and chemical technologies, as a solution to the problems of thermal energy and ecology. In this research, the complex combustion process must be analyzed depending on the influence of numerous physical and chemical parameters of the combustion reaction.

The progress of the formation of liquid droplets theory under high turbulence has a special interest in the study of phenomena in multiphase systems. Research in this area is motivated primarily by environmental problems, in part by problems of atmospheric pollution formation containing toxic heavy metals, sulfuric acid, nitric acid, and other harmful substances.

Reacting systems involve the interaction between several processes occurring simultaneously over a wide range of time and space scales. The release of chemical energy during combustion generates pressure, temperature, and density gradients, which are sources of processes in gases, leading to the transfer of droplets' mass, medium momentum, and the system's internal energy. The strong and ambiguous interaction between the dynamics of liquids and gases and the chemical reactions in them seriously complicates both the experimental study of reacting flows and the development of any more or less rigorous theory. Therefore, numerical simulation can successfully predict and study the behavior of such complex systems. Experimental observations and approximate theoretical models provide laws that an open physical system is supposed to obey. With the help of numerical experiments, it is possible to check the fulfillment of these laws [7].

Methods of mathematical modeling are widely used in various fields of science and technology. These methods include the development of physical and mathematical models, numerical methods and

software, and numerical experiments involving computer technology. Its results are analyzed and used for practical purposes. In science and technology, the advantages of the computer simulation method are obvious: design optimization, reduction of development costs, product quality improvement, operating costs reduction, etc. Numerical modeling also significantly transforms the very nature of scientific research, establishing new forms of the relationship between experimental and mathematical methods.

In this way, the study of spray, dispersion, and evaporation of liquid droplets under high turbulence is an urgent problem that can be solved by computer numerical simulation methods.

2 Mathematical model of the problem

The mathematical model of liquid fuels' atomization and combustion processes in the combustion chamber is based on the equations of motion for the liquid phase accompanied by droplets evaporation, as well as on the equations of energy and mass transfer with appropriate initial and boundary conditions.

The continuity equation for the m component is written as follows [8, 9]:

$$\begin{aligned} \frac{\partial \rho_m}{\partial t} + \vec{\nabla}(\rho_m \vec{u}) = \\ = \vec{\nabla} \left[\rho D \vec{\nabla} \left(\frac{\rho_m}{\rho} \right) \right] + \dot{\rho}_m^c + \dot{\rho}^s \delta_{m1}, \end{aligned} \quad (1)$$

where ρ_m is m component's mass density, ρ is the density of total mass, and u is liquid velocity. After summing equation (1) overall phases, the continuity equation for the liquid is obtained:

$$\frac{\partial \rho}{\partial t} + \vec{\nabla}(\rho \vec{u}) = \dot{\rho}^s. \quad (2)$$

The momentum transfer equation for the liquid phase is written as [10]:

$$\begin{aligned} \frac{\partial(\rho \vec{u})}{\partial t} + \vec{\nabla}(\rho \vec{u} \vec{u}) = \\ = - \frac{1}{a^2} \vec{\nabla} p - A_0 \vec{\nabla} \left(\frac{2}{3} \rho k \right) + \vec{\nabla} \vec{\sigma} + \vec{F}^s + \rho \vec{g}, \end{aligned} \quad (3)$$

where p is fluid pressure. The value of A_0 is zero for laminar flows and unity for turbulent flows.

The viscous stress tensor has the following form [11]:

$$\sigma = \mu[\vec{v}\vec{u} + (\vec{v}\vec{u})^T] + \lambda\vec{v}\vec{u}\vec{l}. \quad (4)$$

The equation of internal energy is as follows [12]:

$$\frac{\partial(\rho\vec{l})}{\partial t} + \vec{v}(\rho\vec{u}\vec{l}) = -\rho\vec{v}\vec{u} + (1 - A_0)\vec{\sigma}\vec{v}\vec{u} - \vec{v}\vec{j} + A_0\rho\varepsilon + \dot{Q}^c + \dot{Q}^s. \quad (5)$$

The heat flux vector \vec{J} is determined by the relation:

$$\vec{j} = -K\vec{v}T - \rho D \sum_m h_m \vec{v}(\rho_m/\rho), \quad (6)$$

where T is liquid temperature, h_m is the enthalpy of the m component, \dot{Q}^c is the source term due to heat released by a chemical reaction, and \dot{Q}^s is heat brought by injected fuel.

The models with two differential equations are more versatile in engineering calculations of turbulent flows and are most commonly used in technical flows. It is a $k - \varepsilon$ model where two equations are solved: for the kinetic energy of turbulence k and its dissipation rate ε [13-15]:

$$\rho \frac{\partial k}{\partial t} + \rho \frac{\partial \bar{u}_j k}{\partial x_j} = \frac{\partial}{\partial x_j} \left[\left(\mu + \frac{\mu_t}{\sigma_k} \right) \frac{\partial k}{\partial x_j} \right] \frac{\partial \bar{u}_i}{\partial x_j} + G - \frac{2}{3} \rho k \delta_{ij} \frac{\partial \bar{u}_i}{\partial x_j} - \rho \varepsilon, \quad (7)$$

$$\begin{aligned} \rho \frac{\partial \varepsilon}{\partial t} + \rho \frac{\partial \bar{u}_j \varepsilon}{\partial x_j} - \frac{\partial}{\partial x_j} \left[\left(\mu + \frac{\mu_t}{\sigma_\varepsilon} \right) \frac{\partial \varepsilon}{\partial x_j} \right] = \\ = c_{\varepsilon_1} \frac{\varepsilon}{k} G - \left[\left(\frac{2}{3} c_{\varepsilon_2} - c_{\varepsilon_3} \right) \rho \varepsilon \delta_{ij} \frac{\partial \bar{u}_i}{\partial x_j} \right] - \\ - c_{\varepsilon_2} \rho \frac{\varepsilon^2}{k}. \end{aligned} \quad (8)$$

These are standard $k - \varepsilon$ equations. Simplicity, good convergence, and good accuracy of the $k - \varepsilon$ model allow it to remain the most used model for modeling a wide range of turbulent flows. This turbulence model is widely used because of its simplicity, savings in computational resources, and sufficient accuracy in predicting the properties of both non-reacting and burning flows. The model works well at high Reynolds numbers and high flow turbulence, which has been successfully applied in many works to calculate the characteristics of a reacting flow with chemical transformations. The values c_{ε_1} , c_{ε_2} , c_{ε_3} , σ_k , σ_ε are model constants that

are determined empirically [16]. The standard values of these constants are often used in calculations of turbulent flows and are determined experimentally.

3 Statistical model of droplet dispersion and breakup under high turbulence

The turbulent flow affects the liquid jet injected into the cocurrent gas jet moving at a relatively high speed, causing liquid droplets to break up. In the case of droplet breakup upon interaction with a gaseous medium, such random processes as the collision of many droplets, turbulence in the liquid, changes in the cavitation inside flow, and promote the process of disintegration of liquid filaments into drops.

The droplets' breakup idea which is proposed by Kolmogorov obeys the cascading law. According to Kolmogorov's theory, the solid particle's breakup is a discrete random process in which the probability of each parent particle's breakup into a certain number of particles does not depend on the size of the original particle itself. From this generalized assumption follows the conclusion that the particles obey the lognormal distribution law. The discrete model of Kolmogorov was modified into the form of a distribution function evolution equation. This equation's asymptotic solution is used in the droplets' breakup and dispersion model along with the Lagrange model, which is also used to describe the spray dynamics [17-20].

We can consider the breakup of parent droplets into small secondary droplets as a temporal and spatial evolution of the particle distribution in approximation to the size of parent particles according to the Fokker-Planck equation [18]:

$$\begin{aligned} \frac{\partial T(x, t)}{\partial t} + v(\xi) \frac{\partial T(x, t)}{\partial x} = \\ = \frac{1}{2} v(\xi^2) \frac{\partial^2 T(x, t)}{\partial x^2}, \end{aligned} \quad (9)$$

where v is breakup frequency and t is breakup time. $T(x, t)$ is distribution function for $x = \ln(r)$, here r is the particle radius.

Since, at high turbulence, the particle sizes far exceed the instantaneous value of the Kolmogorov length scale, and due to the large variety of turbulence kinetic energy spectra, the drops are deformed and destroyed. In this case, the ratio of destructive hydrodynamic and capillary forces determines the critical radius of drops:

$$r_{cr} = \left(\frac{9 We_{cr} \sigma v_{lam}}{\varepsilon \rho_l} \right)^{\frac{1}{3}}. \quad (10)$$

During atomization, the liquid decomposes into a discrete number of particles, each of which is a group of droplets with an identical size, speed, and direction in space. These groups of droplets, dragging the motionless gas along with them, interact with each other and exchange momentum and energy with the surrounding gas. Liquid fuel is injected from the axial nozzle of the injector as discrete particles with characteristic dimensions equal to the radius of the nozzle outlet. The injection rate is determined by the liquid fuel injection. When a particle moves in a

turbulent gas flow with large-scale structures that are much larger than the particle diameter, the relative velocity between the particle and the gas flow is determined:

$$\frac{d\vec{v}_p}{dt} = \frac{(\vec{v}_g - \vec{v}_p)|\vec{v}_g - \vec{v}_p|}{\tau_{St}}, \quad (11)$$

where $\tau_{St} = \frac{\rho_p d_p^2}{18 \rho_g \nu_g}$. When the particle size is larger than the Kolmogorov scale, the turbulent viscosity is governed through the energy spectrum of eddies with smaller sizes compared to the diameter of the particle itself. Figure 2 shows an illustration of this phenomenon.

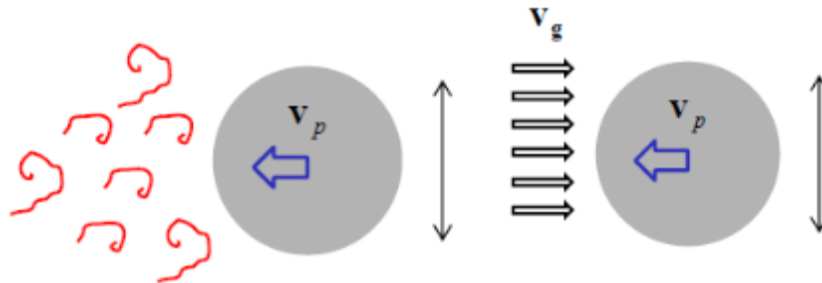


Figure 2 – Comparison of particle sizes with scales of turbulent structures

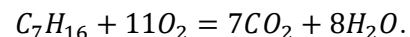
Now we find the change in particle velocity in a turbulent flow:

$$\frac{\bar{v}_g - v_p}{\tau_{St}} = \frac{1}{\varepsilon^{\frac{1}{3}}} \frac{\rho_g}{\rho_p} \frac{\bar{v}_g - v_p}{d_p^{\frac{4}{3}}}. \quad (12)$$

A mixture of fuel and oxidizer is initially injected into the combustion chamber in the form of a continuous jet, which subsequently breaks up into filaments, which in turn into droplets due to interaction with the gas. Due to the mixing of vapors released by floating liquid fragments with a turbulent gas flow, a chemical combustion reaction occurs. If the spray produced does not break up into small droplets, then the mixing process will not be perfect and combustion will not be complete. As a result of this phenomenon, power is lost, additional fuel consumption occurs, and the emission of pollutants into the atmosphere increases. Comprehension of the complex spray formation process and predicting future processes interests engineers, and researchers in fluid mechanics.

4 Physical model of the problem

In this paper, computational experiments were carried out using liquid heptane fuel. The heptane oxidation process in the combustion chamber proceeds as follows:



Heptane is used as a rocket and reference fuel in determining the octane numbers of automobile and aviation types of gasoline and their components by motor and research methods, and the grade of aviation gasoline in a rich mixture. Heptane is a colorless flammable liquid with a flashpoint of minus 4°C and an autoignition temperature of 223°C. The ignition area of heptane vapor in the air is 1.1-6.7% by volume. Heptane refers to the 3rd hazard class and is a paraffinic hydrocarbon. A liquid jet is injected with a high-velocity gas flow into aircraft and rocket engines. This type of disintegration of the fuel into liquid droplets is called air-blast atomization. In this work, the main attention is paid to modeling the

formation and dynamics of the injection during air-blast atomization.

A typical air-blast atomization pattern in aircraft engines is shown in Figure 3 [21, 22]. In such a nozzle, the liquid fuel is injected at low pressure in the form of a thin annular liquid sheet. Two high-

speed air streams go along the fluid and transfer a large amount of kinetic energy. Due to this interaction with the gas stream, the liquid sheet separates from both sides. Thereby, the liquid sheets further break up into bundles, threads, and small droplets.

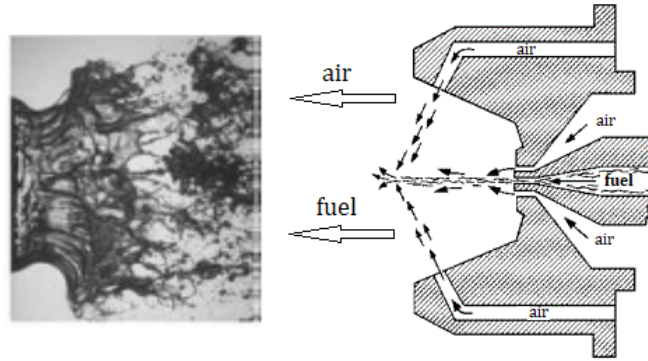


Figure 3 – Scheme of air-blast atomization in an aircraft engine

As can be seen from the figure, the liquid has not yet been fragmented in the nozzle area. This zone, called the liquid core, is a flow region in which the fraction of the mass of the liquid is equal to one, and the bulk of the liquid remains as intact as possible [23]. Many interaction complexes appear at the periphery of the liquid core, which leads to the formation of fibers and their detachment from the liquid core. This liquid core's depletion phase is called primary atomization.

Fragments detached from the liquid core collide with each other. Collisions between fragments can lead to their merging or disintegration. Fragments can also be separated by a fast gas flow that produces small droplets. The phase in which small droplets are produced from large liquid fragments is commonly referred to as secondary atomization. It is clear that the smaller the droplet size, the more intense the evaporation, the better the mixing between the gaseous reactants and, hence, the more efficient combustion. The schematic structure of an aircraft engine is shown in Figure 4.

Liquid fuels' combustion is divided into several stages [24, 25]. At the initial stage, the fuel is injected into the combustion chamber by means of a nozzle into small drops. Before ignition and combustion of the fuel-air mixture, the droplets evaporate and mix with the oxidizer. In the first part of the process, called fuel atomization, the efficiency of the subsequent thorough combustion of the fuel is determined. Since the speed of the processes of

evaporation, mixing of fuel with an oxidizer and subsequent ignition directly depends on the size of the formed droplets. Thus, it becomes possible to realize fast (including supersonic) combustion over relatively short lengths.

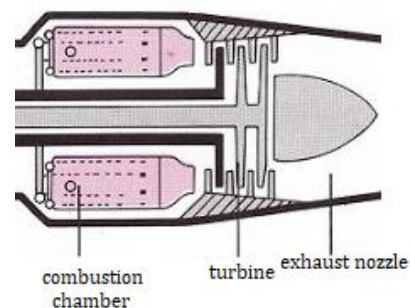


Figure 4 – Schematic structure of an aircraft engine

A combustion zone is established near the drop along a spherical surface, the diameter of which is 1-5 times larger than the droplet size (Figure 5). Droplet evaporation occurs due to the heat of radiation from the combustion zone. In the space between the droplet and the combustion zone, there are vapors of liquid fuel and combustion products. Air and combustion products are in the area outside the combustion zone. Diffusion of fuel vapors occurs inside the combustion zone, while oxygen is outside. Here, these components enter into a chemical reaction, which is accompanied by the release of heat and the formation of combustion products. Heat is

transferred from the combustion zone to the outside and the droplet, while the combustion products diffuse into the surrounding space between the droplet and the combustion zone.

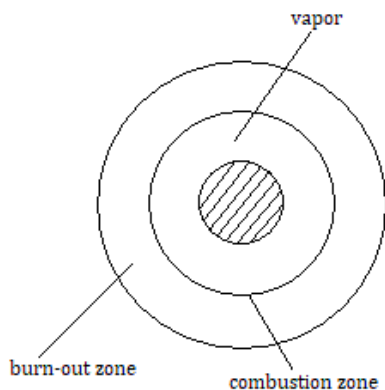


Figure 5 – The thickness of the combustion zone

In our work, when conducting computational experiments, we used a model of a cylindrical combustion chamber. The chamber height is 15 cm, diameter is 4 cm. Figure 6 shows an illustration of the general view of a model combustion chamber. The computational domain consists of 650 cells. Liquid fuel is injected through a nozzle located in the center of the bottom of the combustion chamber. The combustion chamber wall temperature is 353 K.

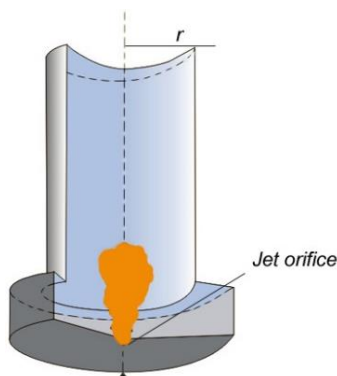


Figure 6 – General view of the combustion chamber

5 Results

This work represents the influence of the liquid fuel injection rate on its combustion using numerical simulation based on the solution of differential two-dimensional equations of a turbulent reacting flow. The injection speed of liquid fuel varied from 150 to 350 m/s. It was found that at low liquid fuel injection rates (less than 150 m/s), combustion does not occur, since in this case the injection rate does not start ignition and stabilize the combustion reaction [26, 27].

The figures below show the results of numerical experiments on the influence of the initial rate of heptane injection in the combustion chamber on the atomization and combustion processes.

Figure 7 shows the combustion temperature distribution in the chamber at different heptane injection rates. Apparently, at an initial speed of 200 m/s the combustion process proceeds slowly and has not become intense. Only at speeds above 250 m/s does the temperature rise along the height of the combustion chamber, the maximum value is 2218 K. Moreover, according to the graph the temperature increases along with the height of the chamber as the injection rate of heptane droplets increases.

The distribution of the temperature plume and the combustion chambers height for heptane is shown in Figure 8. Along with the increase in the droplet injection speed, the height of the plume core increases. For example, at a velocity value of 300 m/s, the maximum temperature propagation area corresponds to a chamber height of 1.7 cm. When particles penetrate the combustion zone along with the chamber height, no noticeable regularity is observed. At a speed value of 250 m/s, the particles rise to a minimum height of 0.56 cm. As a result, it can be said that the speed value at which fuel particles are well dispersed in space is 300 m/s, since at this speed the temperature of particles and intensity of their movements increase, and reach up to 0.81 cm as well as the height of the combustion chamber.

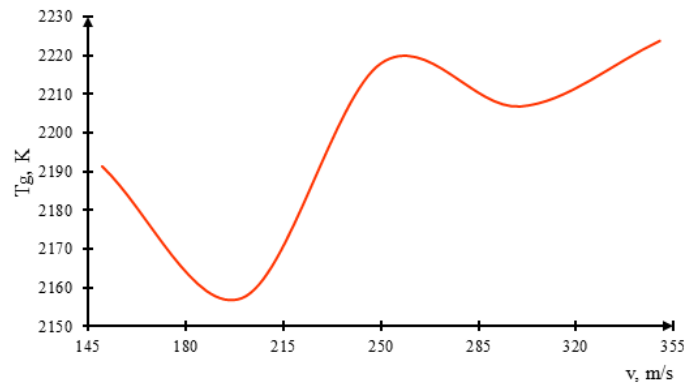


Figure 7 – Dependence of the maximum heptane temperature on the initial droplet injection rate

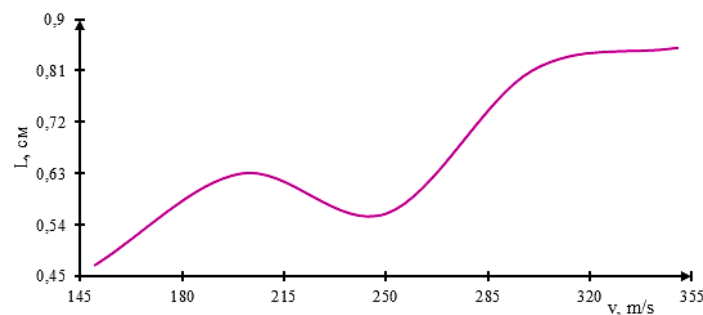


Figure 8 – Distribution of the temperature plume along with the height of the combustion chamber

The Figure 9 shows the concentration distribution of carbon dioxide released in the combustion chamber during the complete oxidation of fuel particles with air. According to the figure, at an initial velocity value of 150 m/s, the CO_2 value is minimal, i.e., 0.128466 g/g. However, as the dispersion rate inside the chamber increases, the intensity of carbon dioxide emission increases. At the speed of 250 m/s, the maximum concentration of carbon dioxide is 0.132253 g/g. The most effective spray velocity at which a moderate carbon dioxide concentration is observed is 300 m/s. At this rate, the CO_2 value is 0.131072 g/g.

Based on the results of the above numerical experiments, the optimal mode of combustion of heptane droplets in the combustion chamber is established at an injection velocity of 300 m/s. At this

velocity value, the temperature inside the chamber reaches a relative maximum value, the intensity of particle breakup and collision increases, and the concentration of carbon dioxide released inside the chamber is relatively lower.

Figure 10 shows the evolution of heptane droplets along the radius in the combustion chamber. At the initial moment of the atomization process (2 ms), the radius of the heptane particles inside the chamber is 3.42 μm . The temperature of the particles increases, and their sizes also begin to change due to collision and breakup processes over time. Particles whose radii are equal to the maximum value (10.515 μm) get congregated at a chamber height of 0.68 cm. At the final moments of combustion, particles of a smaller radius predominate. The particle size value concentrated at the exit from the chamber was 5.355 μm .

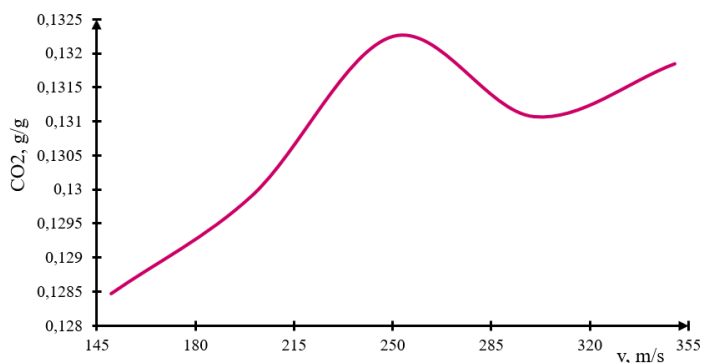


Figure 9 – Distribution of carbon dioxide concentration as a function of injection speed

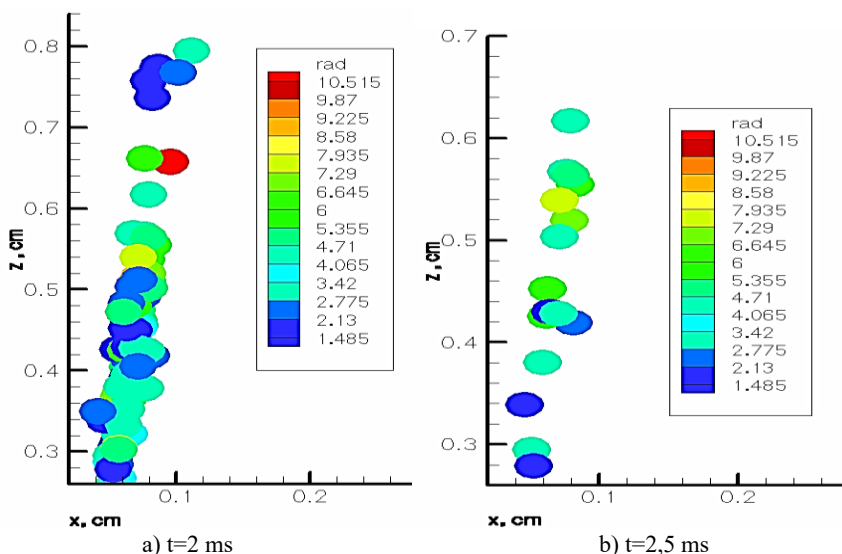


Figure 10 – Dispersion of heptane droplets along with the height of the combustion chamber

Figure 11 shows the heptane’s maximum temperature distribution in the combustion chamber. Liquid fuels maximum combustion temperature at an effective speed of 300 m/s was 2206.84 K. For the rest of the time, a temperature of 1030.39 K was established on the chamber's walls and throughout the combustion space.

The distribution of the concentration of carbon dioxide released in the combustion products is shown in Figure 12. During the combustion process, the concentration of carbon dioxide is allocated uniformly, and any remarkable change is not detected. The minimum concentration of CO₂ at the combustion chamber outlet is 0.0262 g/g.

The distribution of released moisture in the combustion chamber was studied at different times of the entire combustion process (Fig. 13). The moisture

concentration at the initial moment of the combustion process increased to 2 cm along the height of the model combustion chamber. Due to the intensive mixing of the fuel with the oxidizer, as well as the combustion of the fuel, the released moisture in the combustion chamber gradually moves towards its outlet. As we can see from the figure, the maximum concentration of moisture is concentrated on the axis of the combustion chamber, the value of which is 0.057 g/g.

One can see in Figure 14 that by applying the statistical dispersion model, more droplets are heated to a temperature of 500 K than in the base model. Both injections also differ in height. With a statistical model, injection drops reach 1.8 cm in height and 0.5 cm in the radius of the combustion chamber. In the first case, the maximum height of heptane droplets is 1.1 cm.

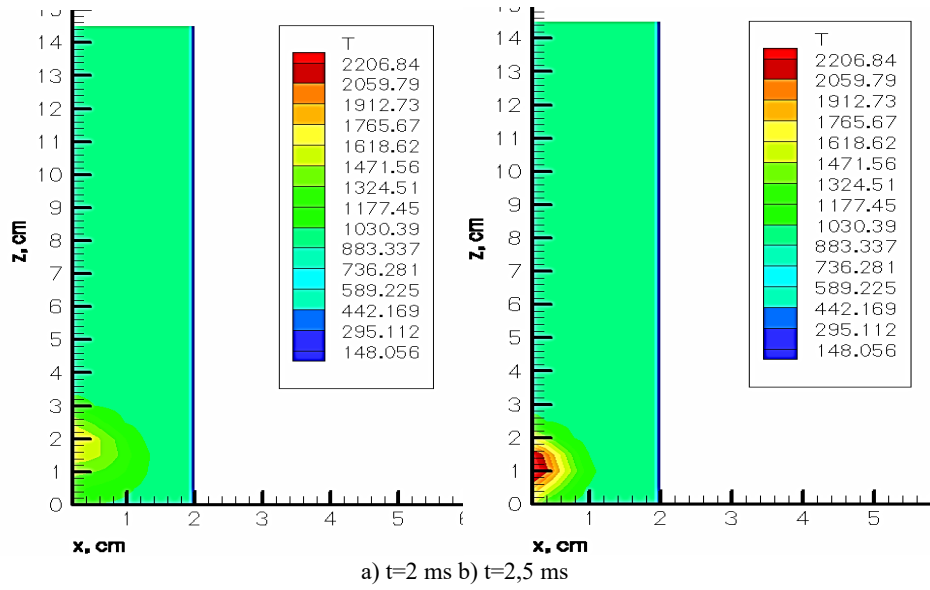


Figure 11 – Distribution of the maximum combustion temperature of heptane along with the height of the chamber

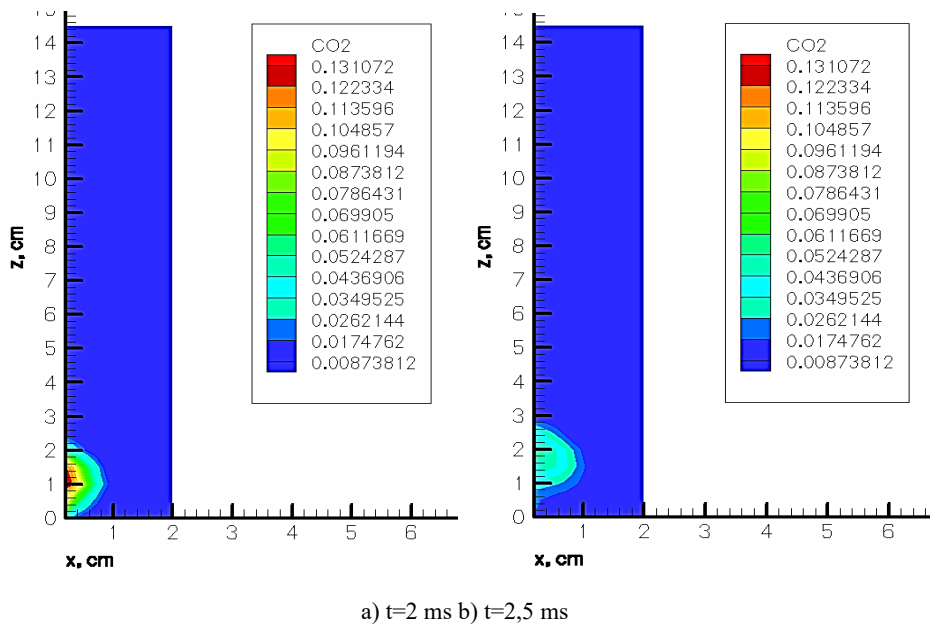


Figure 12 – Concentration profiles of carbon dioxide at different time moments

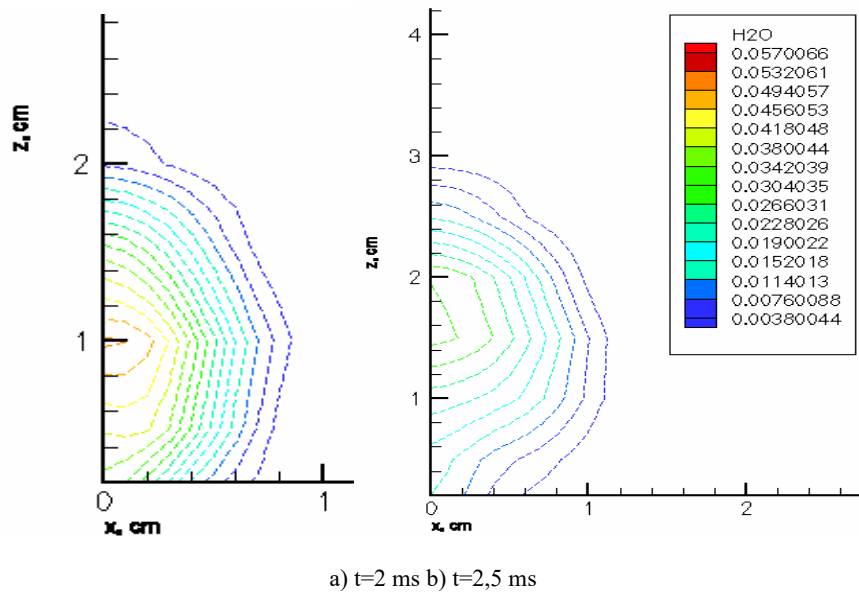


Figure 13 – Water distribution in the combustion chamber

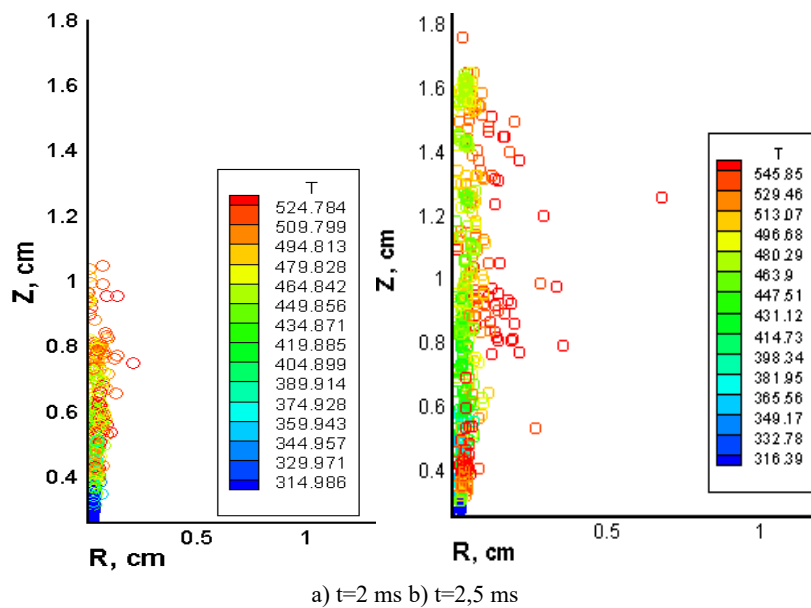


Figure 14 – Dispersion of heptane droplets by specific temperature

Figure 15 shows the size distribution of heptane droplets in the space of the combustion chamber. Heptane particles, whose sizes have a maximum value at the initial time, are concentrated beneath of the chamber, but they evaporate and rise in height over time.

When performing computational experiments, we studied one of the main criteria for the similarity of thermal processes, the Nusselt number, which characterizes the ratio between the intensity of heat

transfer due to convection and the intensity of heat transfer due to thermal conductivity. The Nusselt number is always greater than or equal to 1, the heat flux due to convection always exceeds the heat flux due to heat conduction (Figure 16).

As a result of applying the statistical model in the study of the dispersion and combustion of liquid fuel injections, the droplet distributions in the space of the combustion chamber for heptane were obtained. Taking into account the effect of turbulence on the

dispersion of liquid particles using a statistical model of turbulence in liquid fuel combustion calculations, it was found that liquid fuel droplets are atomized

over a larger volume, which intensifies the liquid fuel combustion process since the mixing of fuel and oxidizer vapors occurs on a more developed surface.

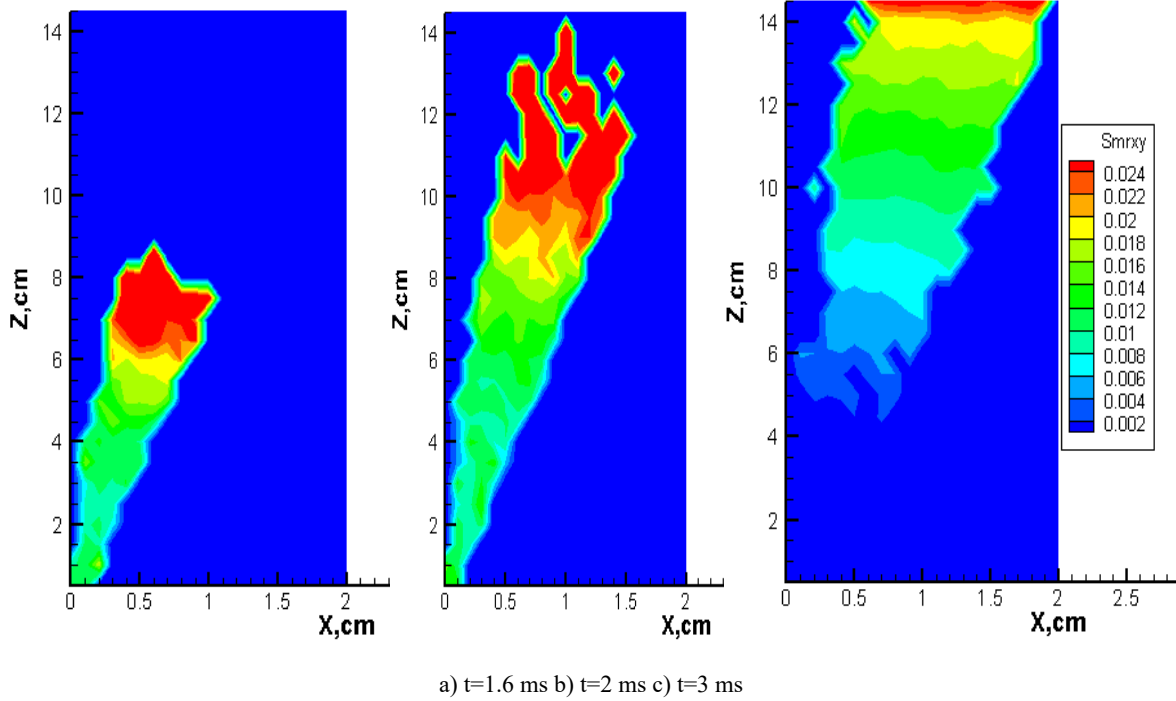


Figure 15 – Dispersion of heptane particles at different time moments

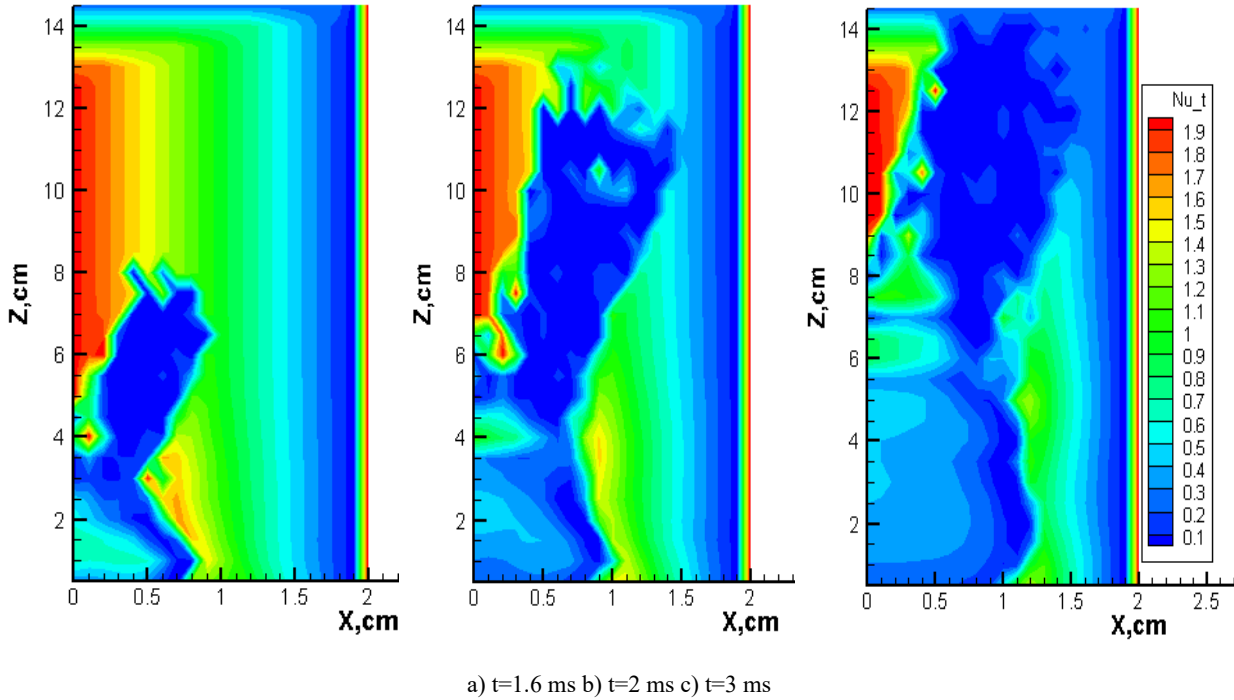


Figure 16 – Nusselt number in the flow at different time moments

Thus, the injection rate influence on the combustion process of heptane in the combustion chamber has been modeled through numerical methods, considering the optimal parameters for the mass of fuel and the initial temperature in the combustion chamber, which were previously determined. The optimum speed for heptane is 300 m/s. The fundamental characteristics of the liquid fuel combustion process are obtained: temperature fields, concentration distributions of fuel and its combustion products, distribution of droplets over radii and temperatures, and velocity fields.

6 Conclusions

The principal features of the combustion of liquid fuel injections are described, and a mathematical model for the formation of dispersion and combustion of non-isothermal liquid injections at high turbulence is presented. The results of a computer experiment on the atomization and combustion of liquid injections using a statistical model are presented. The study of combustion processes depending on the different initial velocities of liquid fuel injection droplets was carried out.

A statistical approach has been proposed to model the dispersion and atomization of liquid fuels in a combustion chamber. The processes of atomization and combustion of heptane injections in a model combustion chamber were studied by means of computational experiments using a statistical model. The distributions of liquid fuel droplets and temperature over time in the space of combustion chamber are obtained.

Due to computational experiments on the injection rate influence on the atomization and combustion of liquid fuel (heptane) processes by using a statistical model, it was found that the optimal combustion mode for heptane occurs at a combustion rate of 300 m/s. At a given speed, the temperature rises, and fuel droplets with an oxidizer react faster and burn without residue.

The theoretical significance of the work is determined by the importance of the results obtained for the development of such branches of knowledge as thermal physics and mechanics of multiphase reacting media. These obtained results will promote to the development of ideas about the regularities of thermophysical processes under the liquid hydrocarbon fuels combustion with continuous supply and the creation of scientific foundations for the development of advanced heat and power technologies.

Using the obtained results in the design of various types of internal combustion engines will simultaneously solve the problems of optimizing the combustion process, increasing the efficiency of fuel combustion and minimizing emissions of harmful substances into the atmosphere. This shows the practical significance of the computational experiments performed in this work.

Acknowledgments

Education and Science Ministry of the Republic of Kazakhstan No. AP14870834 has supported financially this work.

References

1. P. Safarik, et al. Investigation of heat and mass transfer processes in the combustion chamber of industrial power plant boiler. Part 2. Distribution of concentrations of O₂, CO, CO₂, NO // *Journal of Applied and Computational Mechanics*. – 2018. – Vol. 12. – P. 127-138. <http://dx.doi.org/10.24132/acm.2018.396>
2. A. Georgiev, et al. The use of a new “clean” technology for burning low-grade coal in on boilers of Kazakhstan TPPs // *Bulgarian Chemical Communications*. – 2018. – Vol. 50. – P. 53-60.
3. E. Heierle, et al. CFD study of harmful substances production in coal-fired power plant of Kazakhstan // *Bulgarian chemical communications*. – 2016. – Vol. 48. – P. 260-265.
4. Z Liu, P. Ciais, Z. Deng, et al. Near-real-time monitoring of global CO₂ emissions reveals the effects of the COVID-19 pandemic // *Nature Communications*. – 2020. – Vol. 11. – P. 5172. <https://doi.org/10.1038/s41467-020-18922-7>
5. G. Janssens-Maenhout, et al. EDGAR v4.3.2 Global Atlas of the three major Greenhouse Gas Emissions for the period 1970–2012 // *Earth System Science Data*. 2019. – Vol. 11. – P. 959 1002. <https://doi.org/10.5194/essd-2017-79>
6. International Energy Agency (IEA). *Global Energy Review 2020*. (IEA, Paris, 2020). <https://www.iea.org/reports/global-energy-review-2020>.
7. K. Bedikhan, et al. Application of 3D modelling for solving the problem of combustion coal-dust flame // *Bulgarian Chemical Communications*. – 2016. – Vol. 48. – P. 236-241.

8. A. Askarova, N. Slavinskaya, et al. Simulation of non-isothermal liquid sprays under large-scale turbulence // *Physical Sciences and Technology*. – 2021. – Vol. 8, No. 3-4. – P. 28-40. <https://doi.org/10.26577/phst.2021.v8.i2.04>
9. M. Gorokhovski, S.K. Oruganti Stochastic models for the droplet motion and evaporation in under-resolved turbulent flows at a large Reynolds number // *Journal of Fluid Mechanics*. – Cambridge University Press, 2022. – Vol. 932. <https://doi.org/10.1017/jfm.2021.916>
10. P. Safarik, V. Maksimov, et al. 3-D modeling of heat and mass transfer process during the combustion of solid fuel in a swirl furnace // *Acta Polytechnica*. – 2019. – Vol. 59. – P. 543-553. <https://doi.org/10.14311/AP.2019.59.0543>
11. R. Leithner, H. Muller, A. Askarova CFD code FLOREAN for industrial boilers simulations // *WSEAS Transactions on Heat and Mass Transfer*. – 2009. – Vol. 4. – P. 98-107.
12. A. Askarova, et al. Modeling of heat mass transfer in high-temperature reacting flows with combustion // *High Temperature*. – 2018. – Vol. 56. – P. 738-743. <https://doi.org/10.1134/S0018151X1805005X>
13. P. Safarik, A. Nugymanova, et al. Simulation of low-grade coal combustion in real chambers of energy objects // *Acta Polytechnica*. – 2019. – Vol. 59. – P. 98-108. <https://doi.org/10.14311/AP.2019.59.0098>
14. Sh. Ospanova, et al. 3D modelling of heat and mass transfer processes during the combustion of liquid fuel // *Bulgarian Chemical Communications*. – 2016. – Vol. 48. – P. 229-235.
15. V. Maksimov, S. Bolegenova, et al. Mathematical simulation of pulverized coal in combustion chamber // *Procedia Engineering*. – 2012. – Vol. 42. – P. 1150-1156. <https://doi.org/10.1016/j.proeng.2012.07.507>
16. D.C. Amsden, A.A. Amsden The KIVA Story: A Paradigm of Technology Transfer // *IEEE Transactions on Professional Communication Journal*. – 1993. – Vol. 36, Issue 4. – P. 190-195. <https://doi.org/10.1109/47.259956>
17. M. Gorokhovski, V. Saveliev Analyses of Kolmogorov's model of breakup and its application into Lagrangian computation of liquid sprays under air-blast atomization // *Physics of Fluids*. – 2003. – Vol. 15. – P. 184-192. <https://doi.org/10.1063/1.1527914>
18. M. Gorokhovski, R. Zamansky Modeling the effects of small turbulent scales on the drag force for particles below and above the Kolmogorov scale // *Physical Review Fluids*. – 2018. – Vol. 3. – P. 1-23. <https://doi.org/10.1103/PhysRevFluids.3.034602>
19. M. Gorokhovski, A. Barge Effects of regenerating cycle on Lagrangian acceleration in homogeneous shear flow // *Turbulent Cascades II*. – 2019. – Vol. 26. – P. 51-58. https://doi.org/10.1007/978-3-030-12547-9_7
20. M. Beketayeva, et al. Influence of boundary conditions to heat and mass transfer processes // *International Journal of Mechanics*. – 2016. – Vol. 10. – P. 320-325.
21. J. Lasheras, E. Hopfinger Liquid jet instability and atomization in a coaxial gas stream // *Annual Review of Fluid Mechanics*. – 2000. – Vol. 32. – P. 275-308. <https://doi.org/10.1146/annurev.fluid.32.1.275>
22. D. Gao, N. Morley, V. Dhir Numerical simulation of wavy falling film flow using VOF method // *Journal of Computational Physics*. – 2003. – Vol. 192. – P. 624-642. <https://doi.org/10.1016/j.jcp.2003.07.013>
23. J. Helie, M. Gorokhovski, et al. Air entrainment in high pressure multihole gasoline direct injection sprays // *Journal of Applied Fluid Mechanics*. – 2017. – Vol.10. – P. 1223-1234. <http://dx.doi.org/10.18869/acadpub.jafm.73.241.27628>
24. S. Bolegenova, N. Slavinskaya, et al. Investigation of the droplet dispersion influence on the atomization of liquid fuel processes in view of large-scale structures formation // *Recent contributions to physics*. – 2022. – Vol. 80, No. 1. – P. 75-86. <https://doi.org/10.26577/RCPH.2022.v80.i1.09>
26. S. Bolegenova, et al. Investigation of the different Reynolds numbers influence on the atomization and combustion processes of liquid fuel // *Bulgarian Chemical Communications*. – 2018. – 2018. – Vol. 50, Issue G. – P. 68-87.
27. A. Askarova, I. Berezovskaya, et al. Investigation of various types of liquid fuel atomization and combustion processes at high turbulence // *Journal of Engineering and Applied Sciences*. – 2018.- Vol. 13. – P. 4054-4064. <http://dx.doi.org/10.36478/jeasci.2018.4054.4064>